Three Mechanistic Steps Detected by FRET After Presynaptic Filament Formation in Homologous Recombination. ATP Hydrolysis Required for Release of Oligonucleotide Heteroduplex Product from RecA†

Orlando H. Gumbs and Sandra L. Shaner*

Department of Chemistry, Wayne State University, Detroit, Michigan 48202

Received March 20, 1998; Revised Manuscript Received June 24, 1998

ABSTRACT: The *Escherichia coli* RecA protein promotes DNA strand exchange in homologous recombination and recombinational DNA repair. Stopped-flow kinetics and fluorescence resonance energy transfer (FRET) were used to study RecA-mediated strand exchange between a 30-bp duplex DNA and a homologous single-stranded 50mer. In our standard assay, one end of the dsDNA helix was labeled at apposing 5′ and 3′ ends with hexachlorofluorescein and fluorescein, respectively. Strand exchange was monitored by the increase in fluorescence emission resulting upon displacement of the fluorescein-labeled strand from the initial duplex. The potential advantages of FRET in study of strand exchange are that it noninvasively measures real-time kinetics in the previously inaccessible millisecond time regime and offers great sensitivity. The oligonucleotide substrates model short-range mechanistic effects that might occur within a localized region of the ternary complex formed between RecA and long DNA molecules during strand exchange. Reactions in the presence of ATP with 0.1 μM duplex and 0.1−1.0 μM ss50mer showed triphasic kinetics in 600 s time courses, implying the existence of three mechanistic steps *subsequent* to presynaptic filament formation. The observed rate constants for the intermediate phase were independent of the concentration of ss50mer and most likely characterize a unimolecular isomerization of the ternary complex. The observed rate constants for the first and third phases decreased with increasing ss50mer concentration. Kinetic experiments performed with the nonhydrolyzable analogue ATPγS showed overall changes in fluorescence emission identical to those observed in the presence of ATP. In addition, the observed rate constants for the two fastest reaction phases were identical in ATP or ATPγS. The observed rate constant for the slowest phase showed a 4-fold reduction in the presence of ATPγS. Results in ATPγS using an alternate fluorophore labeling pattern suggest a third ternary intermediate may form prior to ssDNA product release. The existence of two or three ternary intermediates in strand exchange with a 30 bp duplex suggests the possibility that the step size for base pair switching may be 10−15 bp. Products of reactions in the presence of ATP and ATPγS, with and without proteinase K treatment, were analyzed on native polyacrylamide gels. In reactions in which only short-range RecA−DNA interactions were important, ATP hydrolysis was not required for recycling of RecA from both oligonucleotide products. Hydrolysis or deproteinization was required for RecA to release the heteroduplex product, but not the outgoing single strand.

The *Escherichia coli* RecA protein is a 38 kDa DNA-dependent ATPase which can catalyze the reciprocal exchange of single strands of DNA between two homologous DNA molecules. It is the most well-understood enzyme that catalyzes recombination and has served as the prototype for studying similar enzymes in prokaryotes and eukaryotes. Understanding the mechanism of RecA-mediated strand exchange is important for providing insights into the ubiquitous cellular processes of DNA recombination and recombinational repair (*1*−*4*). Moreover, this mechanism is important because RecA and other recombinases have potential applications in the area of *in vitro* directed molecular evolution.

A variety of biochemical techniques (filter binding, nuclease assays, electrophoresis, electron microscopy) have been used to characterize the morphology, reaction products, intermediates, and kinetics of the strand-exchange reaction (reviewed in *3*). In these techniques, individual reaction samples must be processed. For kinetic studies, this manipulation constrains the time at which the earliest data point may be determined (≥10 s, depending on technique) and the number and frequency of subsequent data points. Kinetic data have therefore been limited in precision and to processes occurring on a longer time scale (*4*−*8*). In addition, until relatively recently, kinetic studies were performed with long (3−12 kb) natural DNA substrates derived from the single-stranded (ss) or replicative duplex forms of ss bacteriophages (*5*−*7*). Use of long DNA substrates has meant that short-range mechanistic effects involved in strand exchange could not be separated from long-range mechanistic effects such as topological complexities (*9*, *10*).

† Supported by NIH Grant GM47887 to S.L.S.

* Address correspondence to this author. FAX: 313-577-8822. Email: SSH@CHEM.WAYNE.EDU.

S0006-2960(98)00646-1 CCC: $15.00 © 1998 American Chemical Society
Published on Web 07/31/1998

We developed a stopped-flow kinetics method using fluorescence resonance energy transfer (FRET)[1] to study the kinetics of *E. coli* RecA-mediated strand exchange between a 30 bp dsDNA and a homologous ss50mer that is an adaptation of similar spectrophotometric experiments performed with several different helicases (*11*−*13*). Fluorescence resonance energy transfer is the transfer of excited-state energy from a donor fluorophore to an acceptor fluorophore. The rate of transfer depends on the extent of overlap between the emission spectrum of the donor and the absorption spectrum of the acceptor, the relative orientation of the donor and acceptor transition dipoles, and the distance between the two fluorophores (*14*). In our adaptation of this method to the study of the RecA protein, the duplex is typically labeled at the 3′ end of its upper strand with fluorescein and on the 5′ end of its lower strand with hexachlorofluorescein. Overlap between the fluorescence emission spectrum of fluorescein with the excitation spectrum of hexachlorofluorescein results in energy transfer from fluorescein to hexachlorofluorescein and quenching of the fluorescein emission in the duplex. If the upper strand in the duplex is replaced by the incoming homologous strand, the fluorescein emission increases as the fluorescein label is displaced from the proximity of the hexachlorofluorescein. Reaction progress can therefore be followed by monitoring the increase in fluorescein fluorescence as the fluorescein-labeled strand is displaced from the duplex. The advantages of this assay are that it noninvasively measures real-time kinetics in a previously inaccessible time range (milliseconds) and offers greater sensitivity than many other assays currently used.

In addition, we used short oligonucleotides to focus on short-range mechanistic aspects of RecA-mediated strand exchange. The oligonucleotide substrates permit examination of interactions between RecA and the DNA substrates that might occur within a localized region of the extended ternary reaction intermediate formed between RecA and long DNA molecules in strand exchange. This should eliminate mechanistic complications arising from long-range protein−DNA interactions and topological complexities associated with long DNA molecules.

Previous work on the kinetics of RecA-mediated strand exchange between oligonucleotides 83 bases long has used a one-intermediate reaction mechanism to analyze the data (*15*, *16*). We present here kinetic data for strand exchange using a 30 bp oligonucleotide substrate paired with a ss50mer or a ss30mer in reactions with ATP or the nonhydrolyzable analogue, ATPγS. In 10 min time courses in the presence of ATP or ATPγS, a minimum of three distinct mechanistic steps are required *subsequent* to presynaptic filament formation to fit the data adequately. A minimum reaction mechanism consistent with our data appears to require two intermediates:

$$\text{RecA}\cdot\text{ss}_1 + \text{ds}_1 \rightleftarrows \text{I}_1\ (\text{RecA}\cdot\text{ss}_1\cdot\text{ds}_1) \rightleftarrows \text{I}_2\ (\text{RecA}\cdot\text{ss}_2\cdot\text{ds}_2) \rightleftarrows \text{RecA} + \text{ss}_2 + \text{ds}_2$$

where ss_1 and ss_2 are the initial and product ssDNAs, respectively, ds_1 and ds_2 are the initial duplex and the heteroduplex product, and I_1 and I_2 represent different isomeric forms of a ternary complex between RecA and the two homologous DNA substrates. Only the slowest reaction phase observed, with a half-life of about 3 min in the presence of ATP, is affected by the presence or absence of ATP hydrolysis. Results in ATPγS using an alternate fluorophore labeling pattern suggest a third ternary intermediate may form prior to ssDNA product release. The existence of two or three ternary intermediates in strand exchange with a 30 bp duplex suggests the possibility that the step size for base pair switching may be 10−15 bp.

The FRET time courses show that the outgoing fluorescein-labeled strand in the initial duplex is displaced from the near vicinity of its complement in both ATP and ATPγS reactions since energy transfer decreases significantly. The DNA products of ATP and ATPγS reactions not bound to RecA were separated by native polyacrylamide gel electrophoresis, transferred to a nylon membrane, and then identified using structural probes detected by chemiluminescence. The outgoing fluorescein-labeled ss30mer is released by RecA from the ternary nucleoprotein intermediate formed between the homologous ss50mer and the ds30mer with or without ATP hydrolysis. The heteroduplex product is more tightly bound by RecA protein and is released only if ATP is hydrolyzed or the RecA protein is removed by deproteinization in the presence of ATPγS. Previous studies have shown that hydrolysis is needed for recycling RecA from the nucleic acid products (*4*, *17*); however, this is the first demonstration that when only short-range RecA−DNA interactions are considered ATP hydrolysis is required for RecA to release only the newly formed heteroduplex product, not for release of the outgoing single strand.

EXPERIMENTAL PROCEDURES

Buffers and Proteins. Buffers were made with reagent-grade chemicals using distilled water deionized from a Labconco WaterPro PS system. Strand-exchange reactions were performed in buffer T which contained 33 mM Tris-HCl (pH 7.5 at 21 °C) and 23 mM $MgCl_2$. Lactate dehydrogenase, pyruvate kinase, creatine phosphokinase, phosphoenol pyruvate, NADH, phosphocreatine, ATP, and ATPγS were from Sigma.

E. coli RecA protein was purified as described previously (*18*) and stored in 50 mM Tris (pH 8.0 at 21 °C), 0.3 mM EDTA, 5 mM dithiothreitol (DTT), 50% glycerol at −20 °C. Purity was estimated to be ≥95% using Coomassie Blue stained polyacrylamide gels. RecA concentration was determined spectrophotometrically using an extinction coefficient (ϵ) at 277 nm of 2.39×10^4 M^{-1} cm^{-1} (*19*). Purified RecA protein had an ATPase activity of 29 ATP min^{-1} $RecA^{-1}$ at 37 °C using a spectrophotometric ATP hydrolysis assay (*20*). A 500 μL reaction in buffer T containing 0.1 U/μL lactate dehydrogenase, 0.08 U/μL pyruvate kinase, 2 mM phosphoenol pyruvate, 356 μM NADH, 1.25 μM RecA, and 1.2 mM ATP was incubated in a 0.5 cm path length cuvette for 5 min at 37 °C. ATP hydrolysis was initiated

[1] Abbreviations: ATPγS, adenosine 5′-*O*-(3-thiotriphosphate); bp, base pair; BSA, bovine serum albumin; CSPD, disodium 3-(4-methoxyspiro{1,2-dioxetane-3,2′-(5′-chloro)tricyclo[3.3.1.1^{3,7}]decan}-4-yl)phenyl phosphate; dsDNA, double-stranded DNA; FRET, fluorescence resonance energy transfer; ssDNA, single-stranded DNA; U, unit(s).

Table 1: Oligonucleotide Sequences

1. F-ss30mer(U)	5′GCACCAGATTCAGCAATTAAGCTCTAAGCC(F)3′
2. H-ss30mer(L)	5′(H)GGCTTAGAGCTTAATTGCTGAATCTGGTGC3′
3. ss50mer	5′GCACCAGATTCAGCAATTAAGCTCTAAGCC T_{20}3′
4. HF-ds30mer	5′GCACCAGATTCAGCAATTAAGCTCTAAGCC(F)3′ 3′CGTGGTCTAAGTCGTTAATTCGAGATTCGG(H)5′
5. H-ds30mer	5′GCACCAGATTCAGCAATTAAGCTCTAAGCC3′ 3′CGTGGTCTAAGTCGTTAATTCGAGATTCGG(H)5′
6. F-ds30mer	5′GCACCAGATTCAGCAATTAAGCTCTAAGCC(F)3′ 3′CGTGGTCTAAGTCGTTAATTCGAGATTCGG5′
7. H-ds50/30mer	5′GCACCAGATTCAGCAATTAAGCTCTAAGCC T_{20}3′ 3′CGTGGTCTAAGTCGTTAATTCGAGATTCGG(H)5′

by addition of excess ssM13, and the decay in absorbance at 340 nm was monitored as a function of time. An ϵ_{340} for NADH of 6.2×10^3 M^{-1} cm^{-1} was used to determine the rate of hydrolysis from the slope of the time course.

Oligonucleotide Reaction Substrates. The sequences and nomenclature of all oligonucleotides used are summarized in Table 1. Single-stranded oligonucleotides, with or without fluorescent labels, were purchased commercially from Ransom Hill Bioscience, Biosource, or Midland Certified Reagent Co. Oligonucleotides were purified in our laboratory by 15% denaturing polyacrylamide gel electrophoresis, eluted from the acrylamide with 0.3 M sodium acetate (pH 5.2), and run through a Sep-pak C18 (Waters, Millipore) reverse-phase chromatography cartridge (*21*). In some instances, oligos were separated from the polyacrylamide by electroelution with a Centriluter and Centricon 3 (Amicon). The ϵ_{260} used for ss30mer(U) (row 1, Table 1) was 3.42×10^5 M^{-1} cm^{-1} (molecule), and that for ss30mer(L) (row 2, Table 1) was 3.15×10^5 M^{-1} (molecule) cm^{-1} (*22*). Contributions of the fluorophores to the absorbance at 260 nm were negligible for the labeled 30mers. The ss50mer was synthesized and purified by Ransom Hill Bioscience. This ss50mer has a 5′ 30-nucleotide sequence identical to the ss30mer(U) and a T_{20} 3′ end (row 3, Table 1). The ϵ_{260} of the 50mer is 4.55×10^5 M^{-1} (strand) cm^{-1} (*22*). Purified single-stranded oligonucleotides were stored in 10 mM Tris-HCl (pH 8.0), 1 mM EDTA at −20 °C.

A 20 μM working stock of duplex DNA was prepared by mixing equal concentrations of complementary ss oligonucleotides in 10 mM Tris-HCl (pH 7.5 at 24 °C), 0.2 M NaCl followed by heating to 70 °C, equilibrating there for 5 min, and then slowly cooling back down to room temperature. Duplexes were stored at −20 °C. Each duplex was analyzed on a native 20% polyacrylamide gel to verify that no excess single strands were present.

Steady-State Fluorescence Data. Steady-state fluorescence measurements were made using a Spex Fluoromax. Concentrations of oligonucleotides and solvent components used in each experiment are specified in the text or figure legends. The excitation wavelength used with the fluorescein-labeled oligonucleotides was 492 nm with a typical band-pass of 1.7 nm, while emission was scanned from 500 to 600 nm with a typical band-pass of 3.4 nm. Band-passes were chosen to optimize the signal intensity from the HF-ds30mer measured by photon counting. Data points were collected at 0.5 or 1.0 nm intervals. Integration times used in photon counting are indicated in the figure legends for the data presented. In some experiments, a 500 nm cut-on filter (Spex KV500) was inserted into the emission path. Fluorescence spectra were corrected by subtraction of the solvent spectra measured at the same condition.

FRET Kinetics. Some kinetic experiments were carried out in the Spex Fluoromax in a 0.7×0.7 cm fluorescence cuvette placed in a thermostated cuvette holder. Two different protocols were used. In one protocol, a mixture containing RecA, dsDNA, an ATP regeneration system (8 mM phosphocreatine, 10 U/mL creatine phosphokinase), 1.4 mM ATP, 2 mM DTT, and 100 μg/mL BSA was incubated in buffer T at 37 °C for 5 min. The reaction was then initiated by adding ssDNA. Data collection was manually triggered. In the second protocol, RecA and ssDNA were incubated for 5 min at 37 °C in buffer T containing the ATP regeneration system and 0.7 mM ATP. Strand exchange was initiated by addition of dsDNA. In these reactions, BSA and DTT were generally excluded from the buffer. Elimination of BSA and DTT had no effect on our observed results. Concentrations of RecA and ds- and ssDNA are noted in the text or figure legend for each experiment. Time courses were followed using an excitation wavelength of 492 nm and an emission wavelength of 520 nm. Band-passes were chosen to optimize the signal, and were typically set to 1.7 and 3.4 nm for the excitation and emission band-passes, respectively. Data were collected by photon counting at time intervals and for integration periods specified in the figure legends of the data presented.

FRET Stopped-Flow Kinetics. The stopped-flow apparatus employed was a Hi-Tech Scientific SF-51. The flow cell of the stopped-flow instrument was linked by fiber optics to the detection system, a Spex Fluoromax. Excitation occurred at 492 nm, and emission was monitored at 520 nm. Excitation and emission band-passes were set at 11 nm. The temperature of the flow cell was maintained at 37 °C by a circulating water bath. Drive syringes were compressed by a pneumatic ram pressurized with nitrogen gas at 70 psi. In the reaction protocol with the standard oligonucleotide substrates, RecA and 1.4 mM ATP were incubated for 5 min with ss50mer in buffer T and a 2× ATP regeneration system in syringe A. In syringe B, the HF-ds30mer was incubated in buffer T. A 500 nm Spex cut-on filter (KV500) was inserted in the emission path in order to minimize light scattering. Data sampling by photon counting occurred every 50 ms, using a 25 ms integration time, for 120 s. A sampling time interval of 25 ms with 12.5 ms integration was used for a few reactions. Rate constants obtained from fitting these data sets were identical to those obtained with the longer sampling interval.

Description of Kinetic Data Analysis. Following data acquisition, time courses were imported into PSI-Plot (Poly Software International, UT) for analysis by least squares regression. Data were fit to the following double exponential equation:

$$F(t) = F_1{*}[1 - \exp(-k_1{*}t)] + F_2{*}[1 - \exp(-k_2{*}t)] + F_0$$

In this equation, k_1 and k_2 are the observed rate constants for the fast and slow phases of the reaction, and F_1 and F_2 are the respective amplitudes of these phases. The parameter F_0 is the initial fluorescence intensity at the onset of the reaction ($t = 0$), and $F(t)$ is the observed fluorescence at time t. All five parameters were fit to the data. In the

experiments with the standard substrates, the fit value of F_0 agreed reasonably well with the experimentally measured value of F_0. A single exponential equation provided a statistically poorer fit to the data. When analyzing the kinetic data from experiments performed in a cuvette with manual mixing, the pre-trigger time before initiation of strand exchange was subtracted from the instrument clock time for each point to obtain the true reaction time, *t*.

Product Characterization by Southern Hybridization and Chemiluminescent Detection. Reaction products for the ATP and ATPγS reactions were separated by native polyacrylamide electrophoresis and analyzed by Southern transfer (*21*). Reactant and product oligonucleotides separated on the gel were identified by using chemiluminescent detection reagents from Boehringer Mannheim. Identity was established on the basis of reactivity to an anti-fluorescein antibody containing alkaline phosphatase and by sequence complementarity to two different oligonucleotides labeled at their 3′ ends with digoxygenin (DIG). These two oligonucleotides, ss30mer-(U) and ss30mer(L), were each 3′ end labeled with DIG-11-ddUTP by using the Boehringer Mannheim Genius 3′-End Labeling Kit. A labeling efficiency ≥95% was obtained for each DNA. After hybridization of one of these oligos to DNA on the membrane, an anti-DIG antibody with attached alkaline phosphatase was applied and allowed to react with DIG-labeled bands on the membrane. Detection of bands for all three structural probes was based on the reaction of alkaline phosphatase with a dioxetane substrate, disodium 3-(4-methoxyspiro{1,2-dioxetane-3,2′-(5′-chloro)-tricyclo[3.3.1.1^{3,7}]decan}-4-yl) phenyl phosphate (CSPD), that results in a chemiluminescent product. All protocols used are essentially as described by the manufacturer.

The experiment was repeated 5 times. For three of the five experiments, a single gel was run, and the three probes were applied consecutively. For the experiment shown here, the reactions were split and processed on two identical gels. One gel was probed consecutively with DIG-ss30mer(U) and the anti-fluorescein antibody, while the other gel was probed only with DIG-ss30mer(L). RecA-mediated strand exchange was carried out at 37 °C in 80 μL reactions in buffer T with 0.7 mM ATP or ATPγS, 1.25 μM RecA, 0.1 μM (molecule) F-ds30mer, 0.1 μM molecule (5.0 μM nucleotide) ss50mer, and the ATP regeneration system. For the ATP reaction, all components except the ss50mer were mixed and incubated at 37 °C for 5 min. The exchange reaction was initiated by addition of the ss50mer. After 35 min, the sample was loaded onto a 10% native polyacrylamide gel. For ATPγS, two identical reactions were run to compare products with or without deproteinization of the reaction. For ATPγS, all components except the F-ds30mer were mixed and incubated at 37 °C for 5 min. Strand exchange was initiated by the addition of F-ds30mer and allowed to proceed for 35 min. One ATPγS reaction was deproteinized with proteinase K (final concentration of 250 μg/mL) for 15 min prior to loading onto the gel. In other repetitions of this experiment, the time for strand exchange was limited to 15 min. The qualitative results obtained from analysis of the shorter reactions were identical to those obtained in this 35 min reaction. Equivalent amounts of free ss50mer, F-ss30mer-(U), heteroduplex product, or F-ds30mer in reaction buffer were also loaded onto each gel. A gel loading solution with 1.25×10^{-2} % Bromophenol Blue and 4% glycerol was added to all samples before loading. Native 10% polyacrylamide gels (14 × 20 cm, 1.5 mm thick) were run at room temperature at 150 V for approximately 2 h in 1× TBE (0.09 M Tris−borate, 1 mM EDTA; *21*). The gel was then submerged in 0.5 N NaOH, 1.5 M NaCl for 30 min and neutralized in 0.5 M Tris-HCl, pH 7.5, 3 M NaCl. DNA was transferred to a positively charged nylon membrane by capillary transfer using 20× SSC [1× SSC is 0.15 M NaCl, 15 mM Na(citrate), pH 7.0] overnight. Subsequently, the membrane was irradiated for 60 s on a transilluminator, rinsed in distilled water, and allowed to air-dry.

Detection of specific gel bands based on sequence complementarity to either of the two DIG-labeled oligonucleotide probes required an initial hybridization step. The membrane was incubated for 4 h at 68 °C in standard hybridization solution (5× SSC, 0.1% *N*-lauroylsarcosine, 0.02% SDS, 1% blocking reagent). After prehybridization, the solution was replaced with hybridization solution containing the DIG-labeled probe (1.34 fmol/μL). Hybridization was carried out for 4 h, then the membrane was washed extensively with 2× wash solution (2× SSC, 0.2% SDS), followed by 0.5× wash solution.

Fluorescein-labeled oligos or hybridized DIG-labeled oligo probes were detected as described by Boehringer Mannheim. Membranes were blocked for 45 min in 1× blocking solution (Boehringer Mannheim) and then incubated for 30 min at room temperature in 1× blocking solution containing 0.075 unit/mL either anti-fluorescein antibody or anti-DIG antibody. Subsequently, the membrane was washed and incubated in detection buffer (100 mM Tris-HCl, pH 9.5, 100 mM NaCl) for 5 min. The membrane was then placed between two transparencies after topical application of CSPD at a concentration of 0.25 mM. The membrane was exposed at room temperature to Kodak Biomax film for various time intervals (3−60 min). After probing with a single antibody detection agent, the membrane was stripped with 0.2 N NaOH, 0.1% SDS at 37 °C for 10 min. The membrane was then rinsed in 2× SSC and probed again with the anti-fluorescein antibody.

RESULTS

Fluorescence Resonance Energy Transfer Occurs between Donor and Acceptor Fluorophores on Opposite Ends of Complementary DNA Strands in a Duplex. We used FRET to monitor RecA-mediated strand exchange between homologous oligonucleotide substrates. The DNA substrates in most reactions were a ss50mer and a homologous 30 bp duplex, HF-ds30mer (see Table 1 for sequences and label positions). The upper strand of the starting HF-ds30mer had fluorescein (the energy donor in the FRET pair) covalently attached to its 3′ end, whereas the complementary strand had hexachlorofluorescein (the energy acceptor) covalently attached to its 5′ end. The wavelengths for maximal excitation and emission for fluorescein are 492 and 520 nm, respectively. For hexachlorofluorescein, $\lambda_{max,ex} = 535$ nm and $\lambda_{max,em} = 550$ nm. The normalized emission spectrum of F-ss30mer(U) and the excitation spectrum of H-ss30mer(L) are shown in Figure 1A. The large spectral overlap between the fluorescein emission and the hexachlorofluorescein excitation makes these two fluorophores useful in FRET studies (*13*). If the two fluorophores are in close proximity

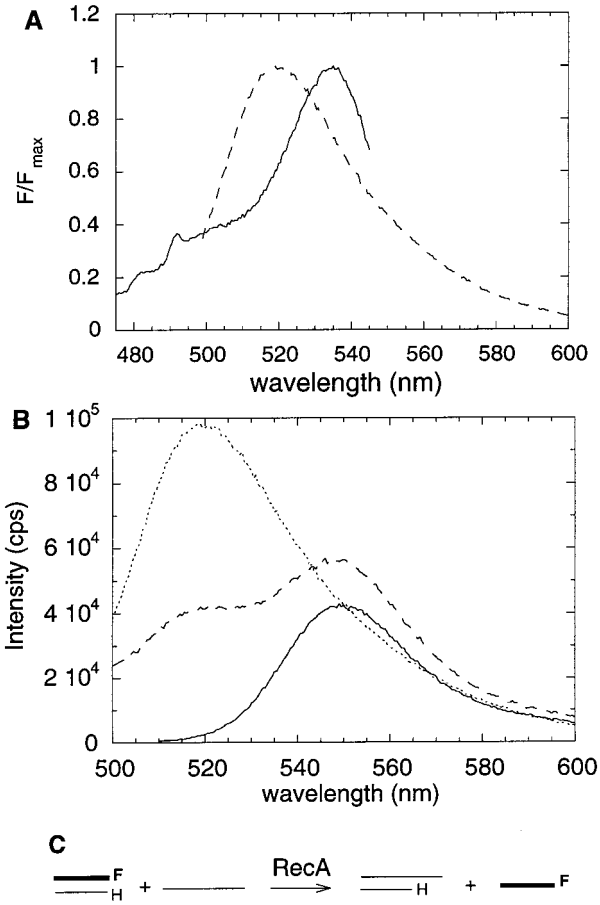

FIGURE 1: Fluorescence properties of the fluorescently labeled DNA substrates used. (A) Comparison of the emission spectrum of F-ss30mer(U) (dashed line) upon excitation at 492 nm with the excitation spectrum of H-ss30mer (solid line) monitored at an emission wavelength of 551 nm. Each spectrum has been normalized to its maximal fluorescence signal. (B) Emission spectra of the F- ss30mer (dotted line), the H-ss30mer (solid line), and the HF-ds30mer (dashed line). Samples were incubated at 21 °C in 20 mM $MgCl_2$, 33 mM Tris-HCl (pH 7.5). Spectra were taken with $\lambda_{ex} = 492$ nm with emission and excitation band-passes of 3.4 and 1.7 nm, respectively. Data were collected every 0.5 nm with 0.25 s integration of the signal. (C) Proposed reaction scheme for strand exchange showing the locations of the fluorescent labels on the reactant and product oligonucleotides.

to each other, energy transfer from fluorescein to hexachlorofluorescein occurs upon excitation of the fluorescein, resulting in increased emission from the hexachlorofluorescein at 550 nm and decreased emission from the fluorescein at 520 nm.

Figure 1B presents the emission spectra of equimolar (molecule) concentrations of separate solutions of the F-ss30mer(U), the H-ss30mer(L), and HF-ds30mer upon excitation at 492 nm. Comparison of the spectra for F-ss30mer(U) and the HF-ds30mer shows that fluorescence emission from the fluorescein decreased from 9.71×10^4 cps to 4.14×10^4 cps due to energy transfer in the duplex. In repeats of this experiment, fluorescence emission from the F-ss30mer(U) was (2.4 ± 0.1)-fold higher than that from an identical concentration of the HF-ds30mer. These spectra indicate that a significant increase in fluorescein emission intensity should accompany strand separation resulting from the RecA protein-mediated strand-exchange reaction. In addition, there is an increase in emission from the duplex observed at 550 nm, the peak of hexachlorofluorescein

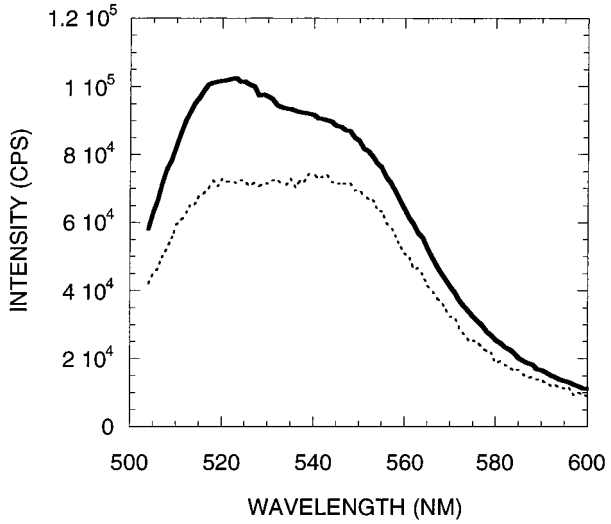

FIGURE 2: Emission spectra before and after strand exchange. RecA protein at 2.5 μM was incubated with 0.1 μM (molecule) HF-ds30mer for 5 min at 37 °C in buffer T containing 1.4 mM ATP, 2 mM DTT, 100 μg/mL BSA, and the ATP regeneration system. Strand exchange was initiated by addition of ss50mer to a final concentration of 0.2 μM strand. The reaction time course was followed by fluorescence emission at 520 nm for 10 min; then a full emission spectrum was taken. The dashed line spectrum is the emission scan of the initial reaction mixture minus the ss50mer, and the solid line spectrum is the emission scan taken 10 min after addition of the ss50mer. The excitation wavelength was 492 nm. Data were collected at 1.0 nm intervals with 0.1 s integration times.

emission. The emission spectrum for H-ss30mer(L) resulting from excitation at 492 nm shows that the hexachlorofluorescein absorbance at that wavelength, although much lower than its absorbance at 535 nm (see Figure 1A), still allows an appreciable emission signal at 550 nm. Importantly, however, the hexachlorofluorescein excitation at 492 nm results in negligible fluorescence emission (2550 cps) at 520 nm, the peak of the fluorescein emission.

The basic experimental design for study of the strand-exchange reaction by FRET is shown in Figure 1C. The HF-ds30mer is allowed to react with presynaptic filaments formed between RecA protein and the ss50mer. The kinetics of the reaction are monitored by detection of the enhanced emission at 520 nm as the fluorescein-labeled upper strand in the starting duplex is displaced by the incoming ss50mer. Oligonucleotides of this size were chosen based on literature reports of the size of the ssDNA needed for efficient use by RecA protein as a cofactor for ATP hydrolysis (*23*, *24*).

RecA-Mediated Strand Exchange Produces a Change in the Fluorescence Spectrum of the Starting DNA Reactants. Prior to looking at the kinetics of strand exchange, steady-state emission spectra were taken at several reaction conditions before and after RecA-mediated strand exchange. In Figure 2, the initial spectrum was measured after incubating a solution of 0.1 μM (molecule) HF-ds30mer and 2.5 μM RecA protein for 5 min at 37 °C. Subsequently, 0.20 μM (molecule) ss50mer was added to the solution with thorough mixing. After 10 min of reaction, the second spectrum was measured. The fluorescence emission at 520 nm increased from 7.28×10^4 cps to 1.02×10^5 cps. The observed enhancement (1.40-fold) of the fluorescein emission at 520 nm is consistent with loss of FRET upon displacement of the F-ss30mer(U) in the duplex by the incoming ss50mer. The enhancement was considerably smaller than the maximal

Table 2: Kinetic Rate Constants for Manual Experiments Performed with 0.1 μM HF-ds30Mer in 0.7 mM ATP at 37 °C

[ss50mer] (μM)	k_2 (s^{-1})	k_3 (s^{-1})	ΔF (%)
0.10	0.025 ± 0.006	0.004 ± 0.001	31.6 ± 5.6
0.15	0.027 ± 0.007	0.0045 ± 0.0007	37.1 ± 4.1
0.20	0.049 ± 0.003	0.0070 ± 0.0002	38.9 ± 2.9
0.25	0.030 ± 0.007	0.004 ± 0.002	46.0 ± 1.0
0.30	0.023 ± 0.002	0.0007 ± 0.0005	52.0 ± 9.0
0.50	0.019 ± 0.004	0.0011 ± 0.0001	61.0 ± 6.0

2.4-fold increase seen when comparing the F-labeled ss30mer to this HF-ds30mer (Figure 1B). Experiments at identical concentrations of RecA protein and oligonucleotides were performed in which RecA and the ss50mer were incubated together first, then followed by duplex addition (Table 2). Here an average enhancement of 39 ± 3% was seen after 10 min of reaction (row 3, Table 2).

In Figure 2, the apparent emission at 550 nm corresponding to the peak of hexachlorofluorescein emission also increased from 6.96×10^4 cps to 8.41×10^4 cps, a factor of 21%. This unexpected increase in the apparent emission at 550 nm was observed with or without the 500 nm cut-on filter in the emission path, although the intensity was higher in the absence of the filter.

For reactions in $Mg(OAc)_2$ in which ss50mer was added last, the fluorescence emission at 520 nm increased 47.2 ± 0.3% relative to its initial starting value. Thus, a slightly larger enhancement occurred in the 520 nm emission for reactions in $Mg(OAc)_2$ compared to ones in $MgCl_2$. This is consistent with prior observation of higher reaction yields in $Mg(OAc)_2$ (*25*).

RecA Protein Binding Quenches the Fluorescence Emission of Free F-ss30mer(U). During RecA protein-mediated strand exchange with the oligonucleotide substrates represented in Figure 1C, the resultant products are hexachlorofluorescein-labeled heteroduplex DNA (row 7, Table 1) and the fluorescein-labeled single-stranded 30mer. The F-ss30mer(U) is a potential target for RecA binding. Quenching of the fluorescein emission might occur upon binding, thus lowering the apparent emission increase associated with displacement of the strand. We compared the emission intensity of 0.1 μM (molecule) F-ss30mer(U) in buffer T containing 0.7 mM ATP at 37 °C in the presence and absence of 0.75 μM RecA protein. The F-ss30mer(U) was incubated at this condition for 5 min prior to taking its emission spectrum. The RecA protein was added to the solution, and the fluorescence emission was followed for 600 s, the maximum time observed in our reaction time courses. The fluorescence quench observed, after correcting for volume changes, in the emission spectrum taken after 10 min was small: 3.0 ± 2.5% (five repeats). The equilibrium value was reached in ≤4 min. When the concentrations of RecA protein and F-ss30mer(U) were increased to 3.75 μM and 0.50 μM, respectively, we saw a corrected quench of 18% (data not shown). Doubling the RecA protein concentration to 7.20 μM at 0.50 μM F-ss30mer(U) increased the fractional quench to 19.7%. Thus, if substantial binding of the displaced F-ss30mer(U) by RecA protein occurs in any of our kinetics experiments, then loss of fluorescence emission intensity would accompany this binding. In our experiments, we tried to minimize the amount of free RecA protein by using one RecA monomer per four nucleotides of the initial ssDNA.

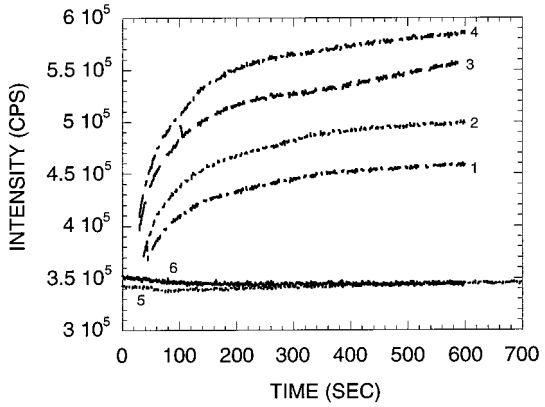

FIGURE 3: Time course of strand exchange in the presence of ATP. Reactions containing RecA and ss50mer were incubated at 37 °C for 5 min in buffer T with 0.7 mM ATP and the ATP regeneration system. Strand exchange was initiated by addition of HF-ds30mer to 0.10 μM (molecule). The time courses shown represent a series of reactions in which the concentrations of ss50mer were raised while maintaining a 4:1 ratio of ss nucleotide to RecA. Concentrations of ss50mer for the reactions shown are 0.10 μM (labeled 1), 0.25 μM (2), 0.30 μM (3), and 0.50 μM (4). The two curves showing negligible time dependence are control reactions in which nonhomologous poly(dT) [12.5 μM (nucleotides); set 5] was used as a heterologous control or in which ss50mer was omitted (set 6) from the reaction. The fluorescence was detected using the following parameters: $\lambda_{ex} = 492$ nm, $\lambda_{em} = 520$ nm, emission and excitation band-pass = 4.25 nm. Data were collected at 1.0 s intervals with 0.5 s integration times.

Kinetics Measured by FRET in Reactions with ATP Hydrolysis. To examine the kinetics of the strand-exchange reaction, we initially measured 600 s time courses for reactions including ATP hydrolysis mixed in cuvettes. Figure 3 shows a series of these reactions in which we maintained the concentration of the HF-ds30mer at 0.10 μM (molecule) and raised the concentration of presynaptic filaments by raising the concentration of the ss50mer from 0.10 μM to 0.50 μM (molecule). The concentration of RecA protein was also raised in order to maintain a constant nucleotide to RecA monomer ratio of 4:1 in each reaction. The RecA and ss50mer were incubated at 37 °C for 5 min in buffer T with 0.7 mM ATP and the ATP regeneration system. Measurements of ATPase activity as a function of $MgCl_2$ concentration using the ss50mer as substrate showed that hydrolysis was optimized at 23 mM, in contrast to the inhibition of hydrolysis at this concentration obtained with long, natural sequence DNAs prone to formation of secondary structure (Gumbs and Shaner, in preparation). At these conditions, ATP hydrolysis measurements with 1.25 μM RecA protein and 0.1 μM ss50mer (5.0 μM nucleotides) showed that about 70% of the protein is bound and hydrolyzing (data not shown). Strand exchange was initiated by addition of HF-ds30mer followed by thorough mixing. Emission data at 520 nm were measured as a function of time and then analyzed by fitting to a double-exponential equation as described under Experimental Procedures. Figure 3 shows that the magnitude of the fluorescence increase accompanying the reaction over the 600 s reaction time course increased from the initial basal level of $(3.45 \pm 0.03) \times 10^5$ cps as the concentration of the ss50mer increases. At 0.10 μM ss50mer, the final fluorescence emission was 4.59

$\times 10^5$ cps, and at 0.50 μM ss50mer, the final emission was 5.87×10^5 cps. This result suggests that the total fluorescence increase is proportional to the final yield and could be used to assess the fractional reaction yield by comparison to the theoretical maximum increase. The average percent increase from the basal level in fluorescence intensity (ΔF) observed after 600 s of reaction at each set of reaction concentrations is shown in Table 2. It rises from 32 to 61% over this 5-fold increase in ss50mer concentration. Experiments were also performed using a 3:1 ss nucleotide to RecA ratio. The increase in fluorescence intensity after 600 s was identical to that observed at the 4:1 ratio.

The basal level fluorescence for this series of reactions was established in control reactions performed in the absence of added ss50mer or with nonhomologous ssDNA [poly(dT)]. These control reactions are also shown in Figure 3. Poly(dT) was used at a concentration of 12.5 μM (nucleotide), identical to the single-stranded nucleotide concentration present in the reaction with 0.25 μM (molecule) ss50mer. For these two control reactions, no significant change in emission at 520 nm was observed from the average basal level, $(3.45 \pm 0.03) \times 10^5$ cps, over 600 s. The reaction with poly(dT) in fact showed no change in emission over 1500 s. Fluorescence emission from control reactions including all reagents except the RecA protein also was unchanged in 400 s of observation. These control reactions demonstrate that the fluorescence emission increase characterizing the full reaction has the correct properties expected for true strand displacement by RecA protein. That is, it requires homologous ssDNA in order to perturb the structure of the starting duplex and displace the original F-ss30mer.

The values obtained for the observed rate constants for each time course when fit to a double-exponential equation are shown in Table 2 for each set of reaction concentrations. Although the increasing amplitude of the observed fluorescence emission indicates that the total reaction yield increased with increasing concentration of presynaptic filament, the values of k_2 showed no dependence on presynaptic filament concentration with an average value of 0.025 ± 0.004 s^{-1}. In contrast, k_3, which has an average value of 0.004 ± 0.001 s^{-1} at 0.1 μM ss50mer, appeared to decrease above 0.25 μM ss50mer. Values of k_2 and k_3 obtained in experiments at 0.1 μM ss50mer were identical within experimental error using a nucleotide to RecA ratio of either 3:1 or 4:1.

By performing these kinetics in a cuvette with manual mixing, we were unable to monitor the first 8−10 s of the strand-exchange reaction. We wished to determine if a faster reaction phase occurred within that time scale that was unmeasurable in the spectrometer. We therefore performed comparable experiments using a stopped-flow apparatus. The experiments, shown in Figure 4, are at reaction conditions *after mixing* identical to those of Figure 3. In this protocol, RecA and the ss50mer at a 1:4 protein to nucleotide ratio were incubated in one syringe in buffer T containing ATP and the ATP regeneration system at 37 °C. Strand exchange was then initiated by mixing this preformed RecA−ssDNA filament with the HF-ds30mer in the other syringe in buffer T. The final concentration of ss50mer was varied from 0.1 to 1.0 μM (molecule), and that of the HF-ds30mer was kept fixed at 0.1 μM. Data points were collected every 50 ms during the first 2 min of the reaction, with 25 ms integration periods. Each data set shown in Figure 4 is an average of four to six reaction time courses performed at a given set of DNA concentrations. As expected based on the manual experiments, the stopped-flow reactions in Figure 4 show that increasing the concentration of presynaptic filaments at a fixed concentration of the HF-ds30mer leads to an overall increase in normalized fluorescence at the end of the 120 s time course. This effect corresponds to an increased yield of product with increasing ss50mer concentration.

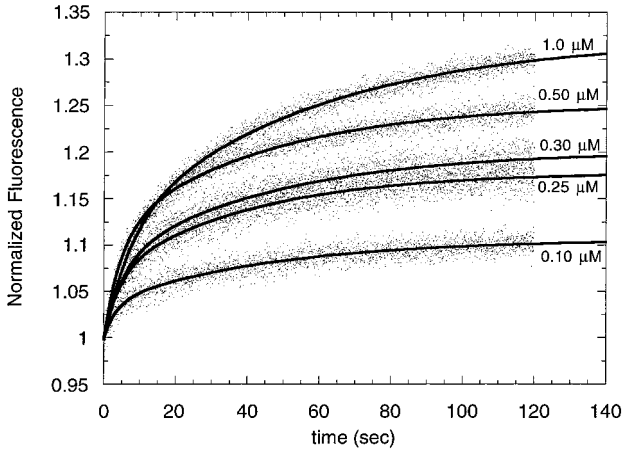

FIGURE 4: Time course of strand exchange in the presence of ATP determined by stopped-flow fluorescence. After mixing, all buffer concentrations are identical to the experiments of Figure 3. Strand exchange was performed at 37 °C with increasing concentration of ss50mer (0.1−1.0 μM) while holding the HF-ds30mer concentration constant. The concentration of the ss50mer used for each data point is shown. The solid lines shown are the best fits to a double-exponential equation. Reaction was monitored at 520 nm with data collection every 50 ms for 2 min.

Averaged time courses were best analyzed by a double-exponential fit, yielding one reaction phase whose half-life was shorter than our mixing time in the manual mixing experiments. The amplitudes and observed rate constants obtained from the fit at each concentration of ss50mer are shown in Table 3. The observed rate constant of the fastest phase (k_1) decreased with increasing ss50mer concentration, decreasing from 0.295 ± 0.033 s^{-1} at 0.10 μM to 0.156 ± 0.015 s^{-1} at 1.0 μM. In contrast, the observed rate constant of the slower phase, k_2, appeared independent of ss50mer concentration as it did in the experiments with manual mixing. The average value of 0.023 ± 0.002 s^{-1} obtained by stopped flow is in excellent agreement with the value of k_2 obtained in the cuvette-based manual mixing experiments. When plotted (not shown), the amplitude of the slower phase, F_2, increased linearly with increasing filament concentration, while that of the fast phase, F_1, increased linearly until an apparent plateau was reached above 0.5 μM ss50mer.

Kinetics Measured by FRET in Reactions with ATPγS. Similar experiments were then performed using ATPγS as the nucleotide cofactor. Since ATP hydrolysis or deproteinization of reaction products was known to be required for recycling of RecA protein from the reaction products (*17*), we expected that reaction progress beyond formation of the ternary nucleoprotein intermediate would be blocked in the absence of ATP hydrolysis. This block might decrease the number of observed reaction phases or slow a particular reaction phase, potentially allowing us to identify reaction phases associated with ATP hydrolysis.

Table 3: Rate Constants and Amplitudes Determined by Stopped-Flow Kinetics for Reactions with 0.7 mM ATP, 0.1 μM HF-ds30Mer at 37 °C

[ss50mer] (μM)	k_1 (s^{-1})	k_2 (s^{-1})	F_1 (cps)	F_2 (cps)	F_0 (cps)	F_1/F_0	F_2/F_0
0.10	0.296 ± 0.033	0.0219 ± 0.0010	6909 ± 381	13116 ± 184	187830	0.037	0.070
0.25	0.236 ± 0.021	0.0253 ± 0.0011	10888 ± 490	18101 ± 341	162490	0.067	0.11
0.30	0.191 ± 0.015	0.0219 ± 0.0012	14099 ± 594	21424 ± 405	176440	0.080	0.12
0.50	0.212 ± 0.008	0.0228 ± 0.0006	20969 ± 399	26670 ± 267	188940	0.11	0.14
1.0	0.156 ± 0.015	0.0210 ± 0.0011	18744 ± 1107	40605 ± 800	185640	0.10	0.22

However, if release of the F-ss30mer(U) were blocked in the presence of ATPγS, then a significantly lower signal might be observed with our standard oligonucleotide substrates. We therefore performed two types of reactions with ATPγS which varied primarily by the positions in which the DNA substrates were labeled with the two fluorophores. In one set of experiments, the standard DNA substrates used in the ATP-containing reactions were used. In the second set of experiments, the F-ss30mer(U) was paired with a singly labeled H-ds30mer (row 5, Table 1), resulting in the HF-ds30mer (row 4, Table 1) as the product heteroduplex. We refer to this set of substrates as the alternate-labeled substrates.

Reactions identical to those in the presence of ATP using the standard DNA substrates, ss50mer and the HF-ds30mer (Figure 1C), were performed in the presence of ATPγS. RecA protein was incubated at 37 °C for 5 min at a concentration of 1.25 μM with 0.1 μM ss50mer (5.0 μM nucleotide) in buffer T, 0.7 mM ATPγS, and the ATP regeneration system. The ATP regeneration system was included to maintain identical solvent conditions in the reactions studied with or without ATP hydrolysis. Strand exchange was then initiated by adding the HF-ds30mer to a final concentration of 0.1 μM (molecule). The time course for this reaction performed in a cuvette with manual mixing is shown in Figure 5C. This reaction is comparable to the 0.10 μM reaction shown in Figure 3 in the presence of ATP hydrolysis. Within 600 s, the fluorescence emission at 520 nm increased by 31.4% over its initial value for this particular reaction. In repeated experiments at this condition, an average increase of 28.5 ± 2.5% was observed. Contrary to the expectation that blocked release of the outgoing strand in the presence of ATPγS would produce a smaller change in fluorescence, the average increase in fluorescence was identical, within experimental error, to the average increase seen at this set of reactant concentrations in the presence of ATP hydrolysis (see row 1, Table 2).

A control reaction in the presence of ATPγS using nonhomologous poly(dT) as the single-stranded DNA substrate is also shown in Figure 5C. There was negligible change in the fluorescence emission signal over the 600 s time course in the absence of homology.

The reactions using the standard oligonucleotide substrates in the presence of ATPγS were best fit to a double exponential. The best fit parameters are summarized in Table 4. Average observed rate constants of $k_2 = 0.019 \pm 0.002$ s^{-1} and k_3 of 0.0011 ± 0.0001 s^{-1} were determined. The observed value of k_2 in this reaction with ATPγS is identical, within experimental error, to that observed in experiments in the presence of ATP. However, the value of k_3 in this reaction appears to be 4 times smaller than the value for k_3 obtained for reactions in the presence of ATP.

A time course using the alternate-labeled oligonucleotide substrates in the strand-exchange reaction with ATPγS is shown in Figure 5A. RecA protein was incubated at 37 °C for 5 min at a concentration of 1.25 μM with 0.1 μM (molecule) F-ss30mer(U) (3.0 μM nucleotide) in buffer T, 0.7 mM ATPγS, and the ATP regeneration system. Strand exchange was initiated by adding 0.1 μM (molecule) H-ds30mer. Figure 5B shows steady-state emission spectra of the reaction before initiating strand exchange and after 600 s of reaction. The peak emission at 520 nm is lower, but an increase in emission is observed at 550 nm due to FRET. Over the 600 s time course, the fluorescence emission at 520 nm dropped from 4.8×10^5 to 4.1×10^5, a decrease of 14.6%. Average kinetic parameters determined from quantitative analysis of duplicate time courses are shown in Table 4. The average value for k_2 is 0.030 ± 0.009 s^{-1}, and the average value of $k_3 = 0.0033 \pm 0.0006$ s^{-1}. Both observed rate constants agree, within experimental errors, with the values determined in reactions using the standard substrates in the presence of ATP hydrolysis (Table 2).

A control reaction containing the alternate-labeled oligonucleotide substrates in the presence of ATPγS in the absence of added RecA protein is also shown in Figure 5A. The initial fluorescence emission in the absence of RecA protein relative to the initial emission from the reaction including RecA protein was larger in magnitude. This result illustrates that binding of RecA to the incoming F-ss30mer(U) occurs under these conditions and results in a 7.7% fluorescence quench in ATPγS. A small decrease of 2.0% was observed over the 600 s time course and can be fit to a single-exponential decay to yield a time constant of 0.0024 ± 0.0002 s^{-1}. The gel experiment described below shows that the F-ds30mer undergoes a minor amount of denaturation at this reaction condition. We therefore believe this protein-independent decrease in fluorescence emission may represent the kinetics of annealing of the F-ss30mer(U) with free H-ss30mer(L) resulting from H-ds30mer denaturation.

Stopped-flow experiments analogous to the experiments shown in Figure 5 using both sets of DNA substrates in the presence of ATPγS were performed in order to characterize the fast reaction phase inaccessible in the cuvette-based kinetic experiments. The averaged data are shown in Figure 6A for experiments using the alternate-labeled DNA substrates and in Figure 6B for experiments using the standard substrates. Averaged time courses were fit to a double-exponential equation. The best fit parameter values are summarized in Table 5. For the reaction in ATPγS using the alternate labeling scheme, $k_1 = 0.31 \pm 0.06$ s^{-1} and $k_2 = 0.026 \pm 0.001$ s^{-1}. Strand exchange with the standard ss50mer and HF-ds30mer was characterized by $k_1 = 0.30 \pm 0.03$ s^{-1} and $k_2 = 0.025 \pm 0.001$ s^{-1}. Within experimental

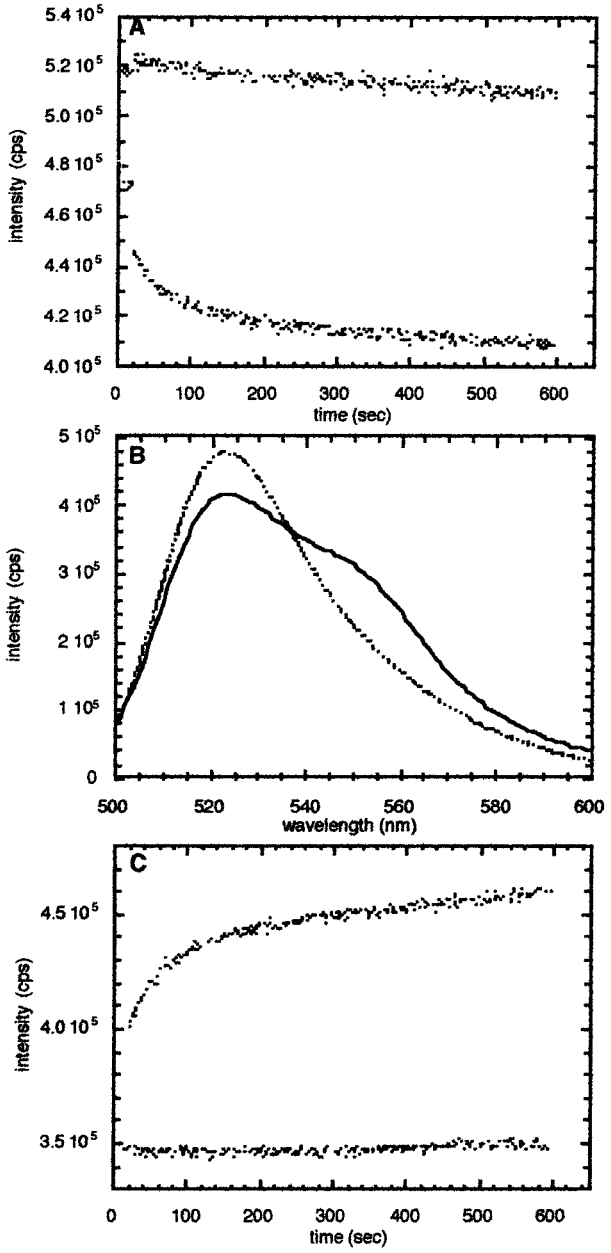

FIGURE 5: (A) Time course of strand exchange in a 'reverse' reaction. RecA was incubated at 37 °C for 5 min at a concentration of 1.25 μM RecA in buffer T, 0.7 mM ATPγS, the ATP regeneration system, and 0.1 μM F-ss30mer(U) (3.0 μM nucleotide). Strand exchange was initiated by adding singly labeled H-ds30mer to a final concentration of 0.1 μM (molecule). A control reaction is shown in which RecA protein was omitted from the reaction. λ_{ex} = 492 nm, λ_{em} = 520 nm. Emission and excitation band-pass = 4.25 nm. Data were collected at 0.5 s intervals with 0.25 s integration periods. (B) Before (dotted line) and after (solid line) emission spectra of the reaction shown in the time course in panel A for full strand-exchange reaction with ATPγS using the 'reverse' substrates. (C) Time course of strand exchange using the 'normal' fluorescently labeled DNA substrates. RecA was incubated at 37 °C for 5 min at a concentration of 1.25 μM in buffer T, 0.7 mM ATPγS, the ATP regeneration system, and 0.10 μM ss50mer (5.0 μM nucleotide). Strand exchange was initiated by adding HF-ds30mer to a final concentration of 0.1 μM (molecule). An identical strand-exchange reaction in which nonhomologous poly(dT) (5.0 μM nucleotide) was used as a heterologous ssDNA is also shown. Instrumental parameters were identical to those in panel A.

error, the two sets of reaction substrates determine identical observed rate constants for each of the two phases. In addition, these values for k_1 and k_2 for reactions in the presence of ATPγS agree with those values obtained at these reactant concentrations using the standard DNA substrates in the presence of ATP hydrolysis (compare Table 5 with row 1 of Table 3).

Table 4: Manual Kinetic Results Using 0.1 μM (Molecule) ssDNA and ds30mer with 0.7 mM ATPγS

	k_2 (s^{-1})	k_3 (s^{-1})	ΔF
standard	0.019 ± 0.002	0.0011 ± 0.0001	28.5 ± 2.5
alternate	0.030 ± 0.009	0.0033 ± 0.0006	16.5 ± 3.5

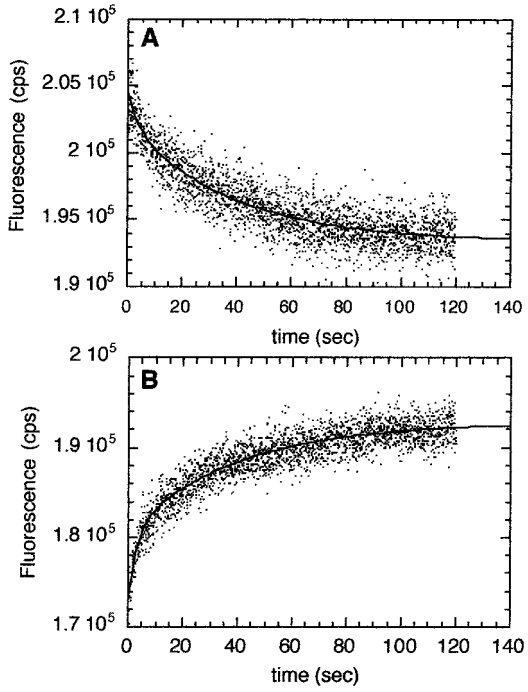

FIGURE 6: Stopped-flow data in the presence of ATPγS. (A) Averaged time course for strand exchange performed at 37 °C using the reverse reaction substrates: F-ss30mer(U) and H-ds30mer. After mixing, the final reaction buffer and reactant concentrations were identical to those in Figure 5A for the reaction with 0.1 μM F-ss30mer(U). Reaction conditions are described in the text. (B) Average time course for the standard strand exchange reaction with 0.1 μM ss50mer and HF-ds30mer in the presence of ATPγS. For each panel, data points were collected every 50 ms with 25 ms integration periods. Data sets shown are the average of four to five stopped-flow experiments. The solid lines shown are the best fits to a double-exponential equation.

Table 5: Stopped-Flow Results for Reactions with ATPγS Using 0.1 μM (Molecule) ssDNA and 0.1 μM (Molecule) ds30Mer

	k_1 (s^{-1})	k_2 (s^{-1})	F_1 (cps)	F_2 (cps)	F_0 (cps)
standard	0.297 ± 0.031	0.0251 ± 0.0011	7453 ± 385	12134 ± 215	173180
alternate	0.308 ± 0.060	0.0260 ± 0.0014	2692 ± 247	8795 ± 186	204800

The fluorescein single-strand product is released from RecA in the presence of ATPγS, while release of the heteroduplex product requires ATP hydrolysis or deproteinization. A number of results in the literature suggest that the nonhydrolyzable ATP analogue, ATPγS, traps joint molecules formed on the reaction pathway for RecA-mediated strand exchange in a triplex intermediate state, with the final reaction products only being released upon deproteinization (*4, 17*). However, in our FRET experiments using the standard oligonucleotide substrates, we see an identical increase in fluorescence emission by the F-ss30mer in the

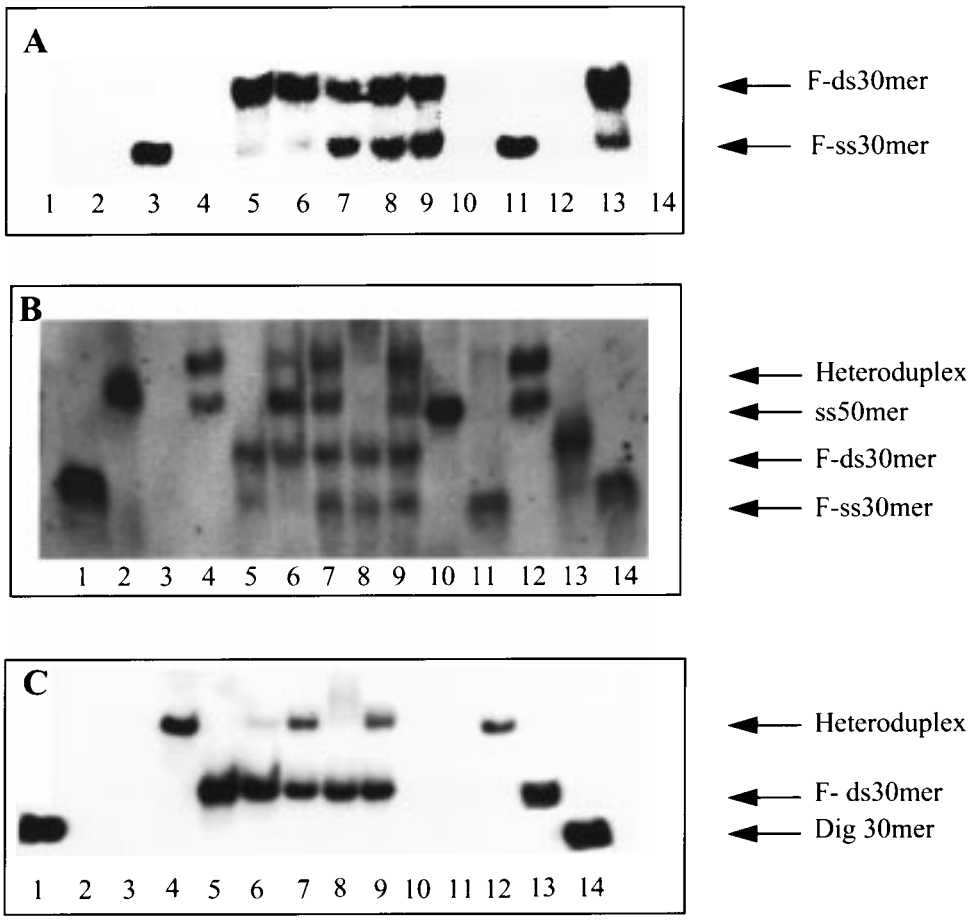

FIGURE 7: Characterization of reaction products by chemiluminescent detection after separation by PAGE and transfer to a nylon membrane. Strand-exchange reactions containing 1.25 μM RecA, 0.1 μM ss50mer, and 0.1 μM F-dsDNA were performed at 37 °C in buffer T in the presence of the ATP regeneration system and 0.7 mM ATP or ATPγS, as indicated. See Experimental Procedures for detailed descriptions of all reaction protocols. Lanes 6−9 contain full strand-exchange reactions varied as follows: ATP without RecA protein, ATP, ATPγS without proteinase K treatment, and ATPγS with proteinase K treatment, respectively. Lanes 1 and 14 contain ssDIG-labeled markers 30 nucleotides long which are not complementary to the oligo probes, but act as controls for reactivity of the anti-DIG antibody. Lanes 2−5 and 10−13 are control lanes to show the mobilities of each free DNA species. The identity of the DNA in each lane is as follows: lanes 2 and 10, 0.1 μM ss50mer; lanes 3 and 11, 0.1 μM F-ss30mer(U); lanes 4 and 12, 0.1 μM heteroduplex product; lanes 5 and 13, 0.1 μM F-ds30mer. After analyzing samples on a 10% polyacrylamide gel, DNA species were transferred to a nylon membrane. Reaction products were identified on the membrane using an anti-fluorescein antibody (panel A) or by hybridization to either DIG-labeled ss30mer(L) (panel B) or DIG-labeled ss30mer(U) (panel C) followed by chemiluminescent detection.

presence of ATP or ATPγS (see Figures 5C and 6B). This implies that either all significant structural changes leading to changes in FRET occur within the ternary intermediate complex or displacement of the F-ss30mer(U) can occur in reactions with ATPγS.

To differentiate between these two possibilities, we compared the products formed in strand-exchange reactions in the presence of ATP hydrolysis with those formed in reactions with the nonhydrolyzable ATPγS, before and after deproteinization of these products by proteinase K. The oligonucleotide substrates used were the ss50mer and the singly labeled F-ds30mer (row 6, Table 1). A detailed description of the reaction and protocols for analysis of the gel bands is found in Experimental Procedures. Reaction mixtures were separated on native polyacrylamide gels and transferred to a nylon membrane. The RecA protein and its complexes with the oligos do not migrate significantly beyond the origin in the gel system used (data not shown); therefore, only species that are not bound by RecA protein are detected. Individual product and starting reagent gel bands were identified on the basis of their relative mobilities and their reactivity with three different structural probes. One structural probe was an anti-fluorescein antibody, with attached alkaline phosphatase, which could bind to any oligo on the membrane containing a fluorescein label. The other two structural probes were DIG-labeled oligonucleotides complementary to the upper and lower strands of the starting ds30mer. Each of these DIG-labeled oligonucleotides could be hybridized to its complement on the membrane. Subsequently, an anti-DIG antibody with attached alkaline phosphatase was allowed to react with the annealed hybrids labeled with DIG. Enzymatic reactions of the alkaline phosphatase allowed chemiluminescent detection of the antibody localized to a particular gel band on the basis of the sequence complementarity to the probe or the presence of fluorescein.

Figure 7 shows the results of the experiment. The reaction schematic in Figure 1C is helpful in understanding what DNA species are expected in a given reaction lane; the one difference is that the duplex used in the gel experiments, F-ds30mer, does not have hexachlorofluorescein on the lower strand as shown in the Figure 1C reaction. Panel 7A depicts

the results obtained with the anti-fluorescein antibody. Gel bands containing the initial F-ds30mer, released F-ss30mer-(U), or any stable fluorescein-containing triplex intermediate will bind to the anti-fluorescein antibody and be detected by the chemiluminescent reaction. The bands that light up in lanes 3 and 11 are the free F-ss30mer(U). Lanes 5 and 13 show the migration position of free F-ds30mer in the gel. A small fraction of the F-ds30mer apparently dissociates at this DNA concentration in the strand-exchange reaction buffer, based on the appearance of a small amount of F-ss30mer(U) running ahead of the duplex in these lanes even though excess single strands were removed from this duplex by gel purification. Lanes 6 and 7 contain ATP strand-exchange reaction mixtures in the absence or presence of RecA protein, respectively, and lanes 8 and 9 contain ATPγS reaction mixtures in the absence or presence of proteinase K, respectively. The released F-ss30mer(U) was prominent in the reactions with ATP (lane 7) and ATPγS (lanes 8 and 9). Deproteinization of the ATPγS reaction was not needed for release of the outgoing strand from the ternary intermediate formed during the reaction with these short oligonucleotides. This observation suggests that the reason the FRET time courses in ATP or ATPγS had comparable fluorescence increases in 600 s was because the F-ss30mer was released from the ternary intermediate in both reactions.

To identify the fate of the heteroduplex product, the membrane was probed with DIG-labeled ss30mer(U). Inspection of Figure 1C and Table 1 shows that this oligo can anneal to any gel bands that contain the complementary sequence of this strand [i.e., ss30mer(L)]. A copy of the sequence of ss30mer(L) is found only in the starting F-ds30mer and the product heteroduplex. Results using this structural probe are shown in panel 7C. Lanes 2, 3, 10, and 11 show no bands because they had no species that hybridize to this probe. Lanes 5 and 13 contain F-ds30mer, while lanes 4 and 12 contain heteroduplex product. The heteroduplex product band migrates significantly slower in the gel than does the F-ds30mer (compare lanes 4 and 5). A band representing heteroduplex product is seen in the full reaction with ATP (lane 7), but not in the reaction with ATPγS without deproteinization (lane 8). Upon addition of proteinase K to the ATPγS reaction (lane 9), the band does appear. These results show either ATP hydrolysis or deproteinization is required for RecA protein to release the bound heteroduplex.

The results from annealing the DIG-labeled ss30mer(L) to DNA on the membrane corroborate the findings with the other two probes and are depicted in panel 7B. This probe anneals to the complementary ss30mer(U) sequence which will appear in the gel bands of the F-ss30mer(U), the ss50mer, F-ds30mer, and the heteroduplex product. Lanes 6−9 contain the reaction mixtures. In the ATP reaction mix in the absence of RecA protein (lane 6), the partial dissociation of the F-ds30mer at this concentration and solution condition (see lane 5) allows some nonenzymatic formation of heteroduplex, resulting in the presence of the heteroduplex band in the protein-free mix and the disappearance of the free F-ss30mer(U). For the full reaction with ATP (lane 7), both the displaced fluorescein strand and the heteroduplex product are visible. In addition, the intensity of the ss50mer band decreases. The ATPγS reactions (lanes 8, 9) both show a band corresponding to released F-ss30mer(U), corroborating the results in panel 7A. In contrast, no free heteroduplex product is present on the gel for the ATPγS reactions unless the reaction is deproteinized before gel loading (compare lanes 8 and 9). This result agrees with the observations using the other oligonucleotide probe in panel 7C. The three structural probes confirm that strand exchange in the presence of ATPγS releases the outgoing strand of this 30 bp initial duplex; however, release of the heteroduplex product by the RecA complex requires either modulation of the binding affinity by ATP hydrolysis or deproteinization by other means.

DISCUSSION

We used FRET to monitor the kinetics of RecA-mediated strand exchange between oligonucleotides at conditions similar to those used in traditional biochemical assays in the presence of ATP or the nonhydrolyzable ATP analogue, ATPγS. In most experiments, DNA substrates in the reactions were a 30 bp duplex, HF-ds30mer, labeled at one end of the helix with both fluorescein and hexachlorofluorescein and a homologous ss50mer. Sequences and label positions are shown in Table 1. In addition, we present results in the presence of ATPγS obtained with an alternate labeling pattern for the oligos in which H-ds30mer was enzymatically paired with a homologous F-ss30mer(U). Experiments were performed in cuvettes or a stopped-flow apparatus.

Kinetic Results in the Presence of ATP or ATPγS. In the presence of ATP hydrolysis, time courses of RecA-mediated strand-exchange reactions between HF-ds30mer and homologous ss50mer were best characterized by three exponential phases *subsequent* to presynaptic filament formation when monitored for 600 s. At 0.1 μM (molecule) ss50mer and HF-ds30mer in ATP, the observed rate constants characterizing each of the three exponential phases were 0.30 $\pm$ 0.03 s^{-1}, 0.022 $\pm$ 0.001 s^{-1}, and 0.004 $\pm$ 0.001 s^{-1}. Since each phase represents a minimum of one mechanistic step (*26*), the reaction mechanism must be represented by a minimum of three steps. The gel experiments in the presence of ATP indicate the outgoing F-ss30mer and the heteroduplex product are both displaced from the RecA; therefore, a minimal reaction scheme consistent with our observations is

$$\mathrm{RecA{\cdot}ss_1} + \mathrm{ds_1} \rightleftarrows \mathrm{I_1\ (RecA{\cdot}ss_1{\cdot}ds_1)} \rightleftarrows \mathrm{I_2\ (RecA{\cdot}ss_2{\cdot}ds_2)} \rightleftarrows \mathrm{RecA} + \mathrm{ss_2} + \mathrm{ds_2} \quad (1)$$

where ss_1 and ss_2 are the initial and product ssDNAs, respectively, ds_1 and ds_2 are the initial duplex and the heteroduplex product, and I_1 and I_2 represent different isomeric forms of a ternary complex between RecA and the two homologous DNA substrates. The observed rate constants determined in the exponential fits to the data will be composites of the individual rate constants characterizing these steps and reactant and intermediate concentrations (*26*). Although the data presented here do not allow us to determine elementary rate constants for particular reaction steps, we can draw a few inferences about the three observed kinetic phases.

The observed rate constant for the second exponential reaction phase was determined by both stopped-flow and

cuvette-based experiments. The measured values of k_2 were in good agreement using either technique, demonstrating that real-time detection of kinetics by FRET can be used effectively without stopped-flow instrumentation to monitor slower processes. In addition, the measured values of k_2 were independent of the concentration of ss50mer, with an overall average value of 0.023 ± 0.002 s^{-1} ($t_{1/2} = 30$ s). Based on this observation, k_2 most likely characterizes the unimolecular isomerization step between intermediates I_1 and I_2 which would be expected to be independent of the initial concentration of presynaptic filament.

The slowest and fastest exponential phases characterizing our time courses in ATP both showed a dependence on the initial concentration of the ss50mer. The initial bimolecular collision step between the presynaptic filament and the duplex should show a first-order dependence on the ss50mer. The observed rate constant characterizing the fastest phase decreased exponentially with increasing concentration of the ss50mer. The kinetic inhibition of this reaction phase by increases in [ss50mer] did not inhibit mass action driving the reaction equilibrium closer to completion since the overall fluorescence emission increased with increasing ss50mer. The ss nucleotide:RecA ratio was maintained at a 4:1 concentration ratio; therefore, the kinetic inhibition cannot be due to a reduction in the concentration of competent presynaptic filaments. The inhibition may result from increased interactions between RecA−ssDNA filaments that compete with productive binding of duplex.

The observed rate constant for the slowest kinetic phase corresponded to a process with a half-life of roughly 170 s below 0.25 μM ss50mer. At higher concentrations of ss50mer, this observed rate constant decreased about 4-fold (Table 2). If the final mechanistic step in which the outgoing F-ss30mer is released were reversible under our conditions, the kinetic data characterizing that step would be affected by the concentration of ssDNA in solution.

To see if elimination of ATP hydrolysis affected the rate constants and amplitudes of any of the observed kinetic phases, we studied strand-exchange reactions in the presence of ATPγS using two different sets of reaction substrates at 0.1 μM (molecule) ss and ds oligonucleotide. Using the alternate-labeled substrates in reactions with ATPγS, the observed rate constants for the three phases were in agreement within error with those determined for the ATP reactions using the standard reaction substrates. In contrast, when using the standard oligonucleotide reaction substrates, the observed rate constants for only the fastest two phases in ATPγS reactions were identical within experimental error to those determined in reactions with ATP. The slowest phase observed in reactions with the standard DNA substrates had a 4-fold smaller observed rate constant in the presence of ATPγS.

Since FRET is dependent upon the distance between the two fluorophores and their relative orientation, one would not expect these two sets of reaction substrates to monitor the kinetics of the exact same mechanistic steps. For the standard substrates in the reaction shown in eq 1, increases in fluorescein emission due to loss of FRET should accompany changes in the orientation and proximity of the two fluorophores at the distal end of the molecule as the two strands are unwound in the ternary intermediate and the upper fluorescein-labeled 30mer is replaced in Watson−Crick base pairing by the incoming ss50mer. Release of F-ss30mer(U) from the ternary intermediate to solution would result in further fluorescence enhancement. In contrast, for the alternate-labeled substrates in the reaction shown in eq 1, decreases in fluorescein emission due to FRET would occur as the ternary intermediate complex forms, initially bringing the F-ss30mer(U) and the H-ds30mer spatially close. Subsequent decreases in emission might be associated with formation of the base-paired heteroduplex HF-ds30mer. With this set of substrates, release of the unlabeled outgoing strand might not be directly observed. Thus, the two different labeling schemes may monitor different steps in the reaction mechanism.

In the reactions with the standard DNA substrates, k_3 is reduced in ATPγS compared to in ATP. However, when the alternate-labeled DNA substrates are used with ATPγS, k_3 is nearly identical to the value determined in the ATP reaction with the standard substrates. We can rationalize these results if the mechanism in eq 1 were modified to include a third ternary intermediate in which the new heteroduplex product is bound to the RecA in its final helical structure while the outgoing single strand is bound but far from the duplex:

$$I_2 \rightleftarrows I_3(\text{RecA}\cdot ds_2 \cdot ss_2) \rightleftarrows \text{RecA}\cdot ds_2 + ss_2 \qquad (2)$$

To account for the observed results, in the ATP reaction k_3 must be dominated by the conversion of I_2 to I_3, with very fast release of ss_2 from I_3. Although the gel experiment showed that the outgoing strand is released by RecA protein in both reactions, it is likely that the affinity of this outgoing strand to the secondary binding site of RecA is tighter in the presence of ATPγS since the affinity of RecA for DNA in the primary site is higher in ATPγS than in ATP. This would result in slower dissociation of ss_2 from I_3 such that k_3 would now reflect this later slower step in ATPγS. The gel experiment showed that the newly formed heteroduplex product was released from the RecA in the presence of ATP hydrolysis, but bound by RecA in the presence of ATPγS. When the alternate-labeled DNA substrates are used, ss_2 has no fluorescein label, and therefore its ultimate displacement should be invisible to detection at 520 nm. Only the I_2 to I_3 conversion would be visible. While the suggestion of a third ternary intermediate in the strand exchange mechanism of the 30 bp oligo is speculative, its existence would explain our results.

One interpretation of the existence of two and possibly three ternary intermediates in strand exchange with this 30 bp duplex is that the step size for cooperative base pair switching is 10−15 bp. The 30 bp duplex would therefore require two or three steps for exchange to be completed. This possible step size gets some support from the observation that RecA can form unstable synaptic complexes with as few as eight bases of homology (*43*). Based on an estimated binding site size of 3.5 ± 0.5 nucleotides or bp per RecA monomer (*1*, *3*), 2−5 RecA monomers would participate in each step of cooperative base pair switching. The Hill coefficient for hydrolysis of ATP by RecA bound to ss- or dsDNA is near 3 (1) and may reflect the minimal size of the RecA protomeric unit involved in each switching step.

Comparison to Previous Kinetic Studies on RecA. Although the known biochemistry of RecA-mediated strand

exchange suggests that the details of the kinetic reaction mechanism will be complex, rigorous study of the kinetics to determine individual rate constants has been technically difficult. The earliest work was limited by use of long DNA substrates and by use of the D-loop assay to determine initial reaction rates (*5*−*7*). Use of long DNA substrates does not permit easy resolution of short-range and long-range mechanistic effects such as topological complexity (*9*, *10*) on the kinetics of the reaction. The D-loop assay detects partially exchanged homologous ternary complexes (joint molecules) retained on a nitrocellulose filter (*27*, *28*). Processing of data points permits collection of data only every 10−15 s, limiting the precision of the observed initial rates. Subsequently, an assay to detect homologous ternary complex formation based on the protection of a restriction site on the initial duplex to restriction digestion was used to characterize the kinetics in ATPγS using DNA substrates varying in length from 27 to 10^9 nucleotides (*8*). Time for enzyme digestion limits the frequency at which data points may be collected in this assay (every 10−15 min), resulting in limited precision of the initial rates.

Conversion of the initial ternary complex into a complex that could be retained on the filter was found to be rate-limiting in the kinetic studies using the D-loop assay (*6*, *7*). Using the enzyme protection assay, initial rates of formation of the homologous ternary complex were found to be first order in the ssDNA and in the dsDNA (*8*). A two-step mechanism was proposed with a steady-state equilibrium forming the initial nonhomologous ternary complex followed by conversion to the homologous ternary complex. Such a mechanism would show second-order kinetics if the conversion to the homologous ternary complex were rate-limiting.

In contrast to this earlier work, we used short oligonucleotides substrates to focus on short-range mechanistic effects in RecA-mediated strand exchange. With a DNA binding site size of 3.5 ± 0.5 ss nucleotides or duplex bp per RecA monomer (*1*, *3*), only 9 ± 2 monomers of RecA will bind to the 30 bp duplex in the ternary intermediate. This corresponds to only 1.5 turns of the RecA protein helix. Use of oligonucleotide reaction substrates should model RecA−DNA interactions which occur within a localized region of the extended ternary complex formed by RecA and long DNA molecules during strand exchange. Mechanistic complications arising from long-range protein−protein and protein−DNA interactions as well as topological problems arising with long duplex DNA will be minimized or completely eliminated.

The most important advantages of a fluorescence-based detection system to monitor strand-exchange kinetics are the high sensitivity and the ability to collect many data points in real time in the earliest period of the reaction. The data presented here were obtained using relatively high concentrations of duplex, 0.1 μM (molecule), because the nucleotide concentration is comparable to nucleotide concentrations used with the older biochemical assays. However, we have performed other reactions with 10 nM (molecule) HF-ds30mer and obtained adequate signal on our instrument (O. H. Gumbs, unpublished results). Previous biochemical assays used to study the kinetics of strand exchange have been limited to slower processes (>10 s) due to constraints of manual mixing or the method of reaction analysis (e.g., *3*, *8*, *20*, *27*−*33*). These assays are unable to identify any mechanistic processes with very short half-lives. FRET stopped-flow kinetics have the potential to be a valuable complement to the traditional assays by providing access to the millisecond time regime.

A further advantage of using FRET to monitor strand-exchange kinetics is seen in our results. The traditional biochemical assays cited previously follow the rate of formation of a single product. We see that multiple reaction steps have an associated change in the energy transfer between the two labeled strands, potentially providing greater mechanistic detail. Further mechanistic information may be accessible by use of different fluorophore labeling strategies.

Radding and colleagues (*16*, *17*, *34*) also recognized the possibilities associated with adapting FRET assays to study of strand exchange. They used a different FRET pair, fluorescein−tetramethylrhodamine, and oligonucleotides that were 83 nucleotides in length. The distance over which energy may effectively transfer is dependent on the choice of the donor−acceptor pair (*14*, *35*). R_0, the distance at which 50% of the energy is transferred, is 45 Å for fluorescein−tetramethylrhodamine (*35*). We were unable to find a literature value for R_0 for the fluorescein−hexachlorofluorescein pair, but it should be larger than 45 Å based on the smaller spectral separation between fluorescein and hexachlorofluorescein. The radius of the RecA nucleoprotein filament is about 50 Å (*3*, *30*, *36*, *37*), with the nucleic acids bound within the protein helix near the longitudinal axis of the filament (*38*, *39*). Although our use of hexachlorofluorescein as acceptor with fluorescein may enable detection of processes that occur over a somewhat longer distance, transfer of the outgoing strand of the initial duplex from the interior of the filament to the exterior should be readily detected by either FRET couple.

Bazemore *et al.* (*15*, *16*) used only a one intermediate reaction mechanism to analyze their FRET kinetic data in reactions with ATP hydrolysis. Since they did not look at reaction times longer than 2 min, they failed to observe the slow reaction phase that we have detected. We can nevertheless compare our values for the observed rate constants of the two faster reaction phases to their values. Using the equivalent of our alternate-labeling pattern for substrates at 0.12 μM (molecule) ss83mer and ds83mer, they determined observed rate constants of 0.3 ± 0.1 s^{-1} and 0.07 ± 0.06 s^{-1} (*15*). These values, within their large error, are in agreement with the values we have obtained in stopped-flow reactions using 0.10 μM (molecule) ss50mer and ds30mer with our standard labeling pattern (Table 3). They also performed experiments using oligonucleotides labeled with the equivalent of our standard labeling pattern. They obtained a better fit to a single exponential for those experiments, and determined that the average observed rate constant was 0.06 ± 0.02 s^{-1} over a 10-fold concentration range in dsDNA. In our experiments with this labeling pattern, we observed a better fit to a double-exponential model based on numerical tests for goodness of fit (lower χ^2 values) as well as by visual comparison of the computed fits with the data.

Comparison of Products with ATP and with the Nonhydrolyzable Analogue, ATPγS. A large literature exists on the role of ATP hydrolysis in strand-exchange reactions of RecA protein and the consequent differences seen in reactions with ATP or ATPγS. A stable triplex intermediate

has been trapped using specialized DNA substrates in RecA-mediated strand exchange (*40*−*43*). Chemical modification and protection experiments have indicated that the incoming strand is placed in the minor groove of the starting duplex (*40*, *44*−*47*). Several experiments have suggested strongly that when strand-exchange reactions are performed in the presence of ATPγS, the three strands assume the hydrogen bonding pattern of the *products* even without release of binding by RecA protein (*44*−*46*, *48*). However, Jain *et al.* (*49*) observed by electron microscopy that when ATPγS was used in RecA reactions only the product heteroduplex was psoralen-cross-linked.

The third strand was displaced or interwound in a conformation that did not permit cross-linking. In contrast, in identical reactions allowing ATP hydrolysis, all three DNA strands in the reaction were cross-linked in a way suggesting dynamic formation of triple-stranded structures. These observations are most compatible with a post-strand switch model for the triplex intermediate (*50*) in which the strands do not need hydrolysis to switch to the product state. In agreement with this, a number of labs have observed that ATP hydrolysis is not necessary for limited strand exchange (*17*, *51*−*53*) and have postulated that the hydrolysis cycle serves merely to modulate the binding affinity of RecA protein for the DNA strands. However, ATP hydrolysis does appear necessary for unidirectional exchange, bypass of structural barriers, four-stranded exchange, and recycling of RecA from the products (*2*, *4*, *17*, *51*, *54*).

We compared RecA strand-exchange reactions performed in ATP or ATPγS using FRET kinetics and gel-product analysis. Identical amplitude changes in the fluorescein emission in the ATP and ATPγS reactions indicated that substantial conformational alterations occur in the ternary complex formed by the initial HF-ds30mer with or without hydrolysis. The affinity of RecA for the product heteroduplex was higher in the presence of ATPγS than in the presence of ATP, since it is only released for migration into the gel after deproteinization in the presence of ATPγS. In contrast, the outgoing single strand of the initial 30 bp duplex was free to migrate into the gel in the presence of ATP or ATPγS, with or without proteinase K treatment. These results mean that the increase in fluorescence seen in the time courses with the standard DNA substrates in the presence of ATP and ATPγS has contributions due to complete displacement of the strand in addition to contributions resulting from structural changes in the starting duplex as base pairs switch within the ternary intermediate. Previous studies have shown that ATP hydrolysis is needed for recycling RecA from the two nucleic acid products (*4*, *17*, *51*). However, this is the first demonstration that ATP hydrolysis is required for RecA to release only the newly formed heteroduplex product, not for release of the outgoing single strand, when only short-range RecA−DNA interactions are considered.

In reactions with longer DNA substrates, complications that are not seen with short oligonucleotides arise from the polymeric structure of the DNAs and the nucleoprotein filament. These complications will slow the kinetics of release of both products from the ternary intermediate. Our results show that an outgoing ss30mer is displaced, even without ATP hydrolysis. With a polymeric outgoing strand, even with simultaneous release of the entire length of the strand by RecA protein, the topological entanglement of the outgoing strand with the nucleoprotein complex between the RecA and the heteroduplex product would slow physical separation of that strand from the RecA−heteroduplex product. This problem is identical to that resulting in the slow kinetics of separation observed between the two strands of T7 DNA when all base pairing is eliminated by high pH (*55*).

Additional origins of the slow release of exchanged products from polymeric reactions may be due to cooperativity of RecA binding to DNA and cooperativity of RecA ATP hydrolysis. Binding of ss or ds DNA to the primary DNA binding site of RecA is highly cooperative (*1*, *3*, *4*). Binding of ssDNA to the secondary DNA binding site of RecA is also cooperative since it was observed to be length dependent (*56*, *57*). The higher binding affinity arising from cooperativity would be expected to slow release of both products. Our results show that a 30 bp heteroduplex is released by RecA protein only if ATP can be hydrolyzed. In strand-exchange reactions between polymeric DNAs, clusters of RecA bound to the heteroduplex that are longer than the number of RecA monomers involved in cooperative ATP hydrolysis would not be synchronized in their release of parts of the heteroduplex. This would result in patches of heteroduplex that are tightly bound to RecA alternating with patches of heteroduplex that have been released locally (*33*, *58*). Released segments in the interior would be more likely to be rebound based on the presence of cooperatively bound proteins on both sides of the patch. This scenario is plausible since exchange between free and bound pools of RecA has been documented for binding to polymeric dsDNA in the presence and absence of strand exchange (*59*, *60*). Stability of binding of RecA to the product heteroduplex appears to depend on the ATP:ADP ratio since binding is maintained for a longer period in the presence of a higher level of ATP regeneration (*48*, *61*). Modulation of the binding stability to the heteroduplex by the local *in vivo* or *in vitro* ATP:ADP ratio may be a mechanism to allow adequate time for separation of the displaced single strand from the heteroduplex so that the round of recombination is not reversed.

REFERENCES

1. Roca, A. I., and Cox, M. M. (1990) *CRC Crit. Rev. Biochem. Mol. Biol. 25*, 415−456.
2. Cox, M. M. (1994) *Trends Biochem. Sci. 19*, 217−222.
3. Kowalczykowski, S. C., and Eggleston, A. K. (1994) *Annu. Rev. Biochem. 63*, 991−1043.
4. Kowalczykowski, S. C. (1991) *Annu. Rev. Biophys. Biophys. Chem. 20*, 539−575.
5. Gonda, D. K., and Radding, C. M. (1983) *Cell 34*, 647−654.
6. Gonda, D. K., Shibata, T., and Radding, C. M. (1985) *Biochemistry 24*, 413−420.
7. Julin, D. A., Riddles, P. W., and Lehman, I. R. (1986) *J. Biol. Chem. 261*, 1025−1030.
8. Yancey-Wrona, J. E., and Camerini-Otero, R. D. (1995) *Curr. Biol. 5*, 1149−1158.
9. Honigberg, S. M., and Radding, C. M. (1988) *Cell 54*, 525−532.
10. Jwang, B., and Radding, C. M. (1992) *Proc. Natl. Acad. Sci. U.S.A. 89*, 7596−7600.
11. Raney, K. D., Sowers, L. C., Millar, D. P., and Benkovic, S. J. (1994) *Proc. Natl. Acad. Sci. U.S.A. 91*, 6644−6648.
12. Houston, P., and Kodadek, T. (1994) *Proc. Natl. Acad. Sci. U.S.A. 91*, 5471−5474.

13. Bjornson, K. P., Amaratunga, M., Moore, K. J. M., and Lohman, T. M. (1994) *Biochemistry 33*, 14306−14316.
14. Lakowizc, J. R. (1983) *Principles of Fluorescence Spectroscopy*, Plenum Press, New York.
15. Bazemore, L. R., Takahashi, M., and Radding, C. M. (1997) *J. Biol. Chem. 272*, 14672−14682.
16. Bazemore, L. R., Folta-Stogniew, E., Takahashi, M., and Radding, C. M. (1997) *Proc. Natl. Acad. Sci. U.S.A. 94*, 11863−11868.
17. Roselli, W., and Stasiak, A. (1990) *J. Mol. Biol. 216*, 335−352.
18. Shibata, T., Cunningham, R. P., and Radding, C. M. (1981) *J. Biol. Chem. 256*, 7557−7564.
19. Tsang, S. S., Muniyappa, K., Azhderian, E., Gonda, D. K., Radding, C. M., Flory, J., and Chase, J. W. (1985) *J. Mol. Biol. 185*, 295−309.
20. Kowalczykowski, S. C., and Krupp, R. A. (1987) *J. Mol. Biol. 193*, 97−113.
21. Sambrook, J., Fritsch, E. F., and Maniatis, T. (1989) *Molecular Cloning: A Laboratory Manual*, 2nd ed., Cold Spring Harbor Laboratory Press, Cold Spring Harbor, NY.
22. Richards, E. G. (1975) in *Handbook of Biochemistry and Molecular Biology: Nucleic Acids*, 3rd ed., Vol. 1, p 597, CRC Press, Cleveland, OH.
23. Brenner, S. L., Mitchell, R. S., Morrical, S. W., Neuendorf, S. K., Schutte, B. C., and Cox, M. M. (1987) *J. Biol. Chem. 262*, 4011−4016.
24. Bianco, P. R., and Weinstock, G. M. (1996) *Nucleic Acids Res. 24*, 4933−4939.
25. Roman, L. J., and Kowalczykowski, S. C. (1986) *Biochemistry 23*, 7375−7385.
26. Johnson, K. A. (1992) *Enzymes (3rd Ed.) 20*, 1−61.
27. Beattie, K. L., Wiegand, R. C., and Radding, C. M. (1977) *J. Mol. Biol. 116*, 783−803.
28. Bianchi, M., DasGupta, C., and Radding, C. M. (1983) *Cell 34*, 931−939.
29. Cox, M. M., and Lehman, I. R. (1981) *Proc. Natl. Acad. Sci. U.S.A. 78*, 3433−3437.
30. Stasiak, A., Stasiak, A. Z., and Koller, T. (1984) *Cold Spring Harbor Symp. Quant. Biol. 49*, 561−70.
31. Bedale, W. A., and Cox, M. M. (1996) *J. Biol. Chem. 271*, 5725−5732.
32. Shaner, S. L., and Radding, C. M. (1987) *J. Biol. Chem. 262*, 9211−9219.
33. Shaner, S. L., Flory, J., and Radding, C. M. (1987) *J. Biol. Chem. 262*, 9220−9230.
34. Gupta, R. C., Bazemore, L. R., Golub, E. I., and Radding, C. M. (1997) *Proc. Natl. Acad. Sci. U.S.A. 94*, 463−468.
35. Selvin, P. R. (1995) *Methods Enzymol. 246*, 300−334.
36. Flory, J., and Radding, C. M. (1982) *Cell 28*, 747−756.
37. Williams, R. C., and Spengler, S. J. (1986) *J. Mol. Biol. 187*, 109.
38. Leahy, M. C., and Radding, C. M. (1986) *J. Biol. Chem. 261*, 695−660.
39. Egelman, E. H., and Stasiak, A. (1986) *J. Mol. Biol. 191*, 677−697.
40. Rao, B. J., Dutreix, M., and Radding, C. M. (1991) *Proc. Natl. Acad. Sci. U.S.A. 88*, 2984−2988.
41. Rao, B. J., and Radding, C. M. (1993) *Proc. Natl. Acad. Sci. U.S.A. 90*, 6646−6650.
42. Rao, B. J., and Radding, C. M. (1994) *Proc. Natl. Acad. Sci. U.S.A. 91*, 6161−6165.
43. Hsieh, P., Camerini-Otero, C. S., and Camerini-Otero, R. D. (1992) *Proc. Natl. Acad. Sci. U.S.A. 89*, 6492−6496.
44. Adzuma, K. (1992) *Genes Dev. 6*, 1679−1694.
45. Baliga, R., Singleton, J. W., and Dervan, P. B. (1995) *Proc. Natl. Acad. Sci. U.S.A. 92*, 10393−10397.
46. Podyminogin, M. A., Meyer, R. B., and Gamper, H. B. (1995) *Biochemistry 34*, 13098−13108.
47. Jain, S. K., Inman, R. B., and Cox, M. M. (1992) *J. Biol. Chem. 267*, 4215−4222.
48. Ullsberger, C. J., and Cox, M. M. (1995) *Biochemistry 34*, 10859−10866.
49. Jain, S. K., Cox, M. M., and Inman, R. B. (1995) *J. Biol. Chem. 270*, 4943−4949.
50. Burnett, B., Rao, B. J., Jwang, B., Reddy, G., and Radding, C. M. (1994) *J. Mol. Biol. 238*, 540−554.
51. Menetski, J. P., Bear, D. G., and Kowalczykowski, S. C. (1990) *Proc. Natl. Acad. Sci. U.S.A. 87*, 21−25.
52. Rehrauer, W. M., and Kowalczykowski, S. C. (1993) *J. Biol. Chem. 268*, 1292−1297.
53. Kowalczykowski, S. C., and Krupp, R. A. (1995) *Proc. Natl. Acad. Sci. U.S.A. 92*, 3478−3482.
54. Shan, Q., Cox, M. M., and Inman, R. B. (1996) *J. Biol. Chem. 271*, 5712−5724.
55. Wensley, C. G., and Record, M. T., Jr. (1975) *Biopolymers 15*, 717−728.
56. Mazin A. V., and Kowalczykowski, S. C. (1996) *Proc. Natl. Acad. Sci. U.S.A. 93*, 10673−10678.
57. Mazin A. V., and Kowalczykowski, S. C. (1998) *EMBO J. 17*, 1161−1168.
58. Lindsley, J. E., and Cox, M. M. (1989) *J. Mol. Biol. 205*, 695−711.
59. Shan, Q., and Cox, M. M. (1997) *J. Biol. Chem. 272*, 11063−11073.
60. Shan, Q., and Cox, M. M. (1996) *J. Mol. Biol. 257*, 756−774.
61. Pugh, B. F., & Cox, M. M. (1987) *J. Biol. Chem. 262*, 1337−1343.

BI980646S